Chinese Journal of Chemical Engineering 60 (2023) 228–234

Contents lists available at ScienceDirect

Chinese Journal of Chemical Engineering

journal homepage: www.elsevier.com/locate/CJChE

Full Length Article

Kinetic mechanism of copper extraction from methylchlorosilane slurry residue using hydrogen peroxide as oxidant

Xiaolin Guo [1], Zhaoyang Zhang [1], Pengfei Xing [1,*], Shuai Wang [1], Yibing Guo [2], Yanxin Zhuang [3]

[1] School of Metallurgy, Northeastern University, Shenyang 110819, China
[2] Ecological Environmental Monitoring Center of Liaoning Province, Shenyang 110819, China
[3] School of Materials Science and Engineering, Northeastern University, Shenyang 110819, China

ARTICLE INFO

Article history:
Received 14 October 2022
Received in revised form 6 February 2023
Accepted 9 February 2023
Available online 15 February 2023

Keywords:
Methylchlorosilane slurry residue
Copper extraction
Hydrogen peroxide
Kinetics

ABSTRACT

Copper was extracted from methylchlorosilane slurry residue by a direct hydrogen peroxide leaching method. A number of experimental parameters were analyzed to determine the extraction efficiency of copper. The extraction efficiency of copper reached 98.5% under the optimal leaching conditions, such as the hydrogen peroxide concentration of 1.875 mol·L^{-1}, the leaching temperature of 323 K, the liquid–solid ratio of 20 ml·g^{-1}, and the stirring speed of 300 r·min^{-1}. The leaching kinetics of the copper extraction process was then described by the shrinking core model. There were two stages. The first stage was controlled by chemical reactions, while the second stage was controlled by interface transfer and product layer diffusion. The activation energy and kinetic control equations were determined, as well as an explanation of the leaching mechanism of copper extraction based on kinetic analysis and materials characterization. Copper resources can be recovered from the methylchlorosilane slurry residue efficiently and inexpensively with the methods used in this study.

1. Introduction

Organosilicon with some organic groups directly attached to the silicon atom is extensively used for a number of applications because of great performance, safety and reliability [1,2]. The direct synthetic reaction [3] is the most economical and effective process for preparing organosilicon monomers, usually methylchlorosilane [4]. Silicon powders react with methyl chloride (CH_3Cl) gas to obtain methylchlorosilanes catalyzed Cu-based catalysts. Many byproducts are produced in this process including methylchlorosilane slurry residue (MSR). There are organosilicon with a boiling point above 473 K, unreacted silicon, reduced activity copper and a small amount of other metals. A methylchlorosilane plant with a 60 kt·a^{-1} capacity will generate about 2 kt·a^{-1} of MSR. Strong acids and acid mist are generated if the MSR is open-air preserved [5]. The disposal methods of MSR are mainly landfill and incineration, which not only poses a threat to the environment, but also wastes copper and other valuable resources [6]. It is therefore necessary to recover copper from MSR so as to produce copper-containing chemicals as well as to maximize resource usage, which is crucial for promoting green and sustainable development in the organosilicon industry.

Since copper is mainly derived from Cu–Cu_2O–CuO catalysts, the presence of copper is more complex, mainly monovalent copper, divalent copper and monomers. The total copper mass contents range from 5% to 8%, which is higher than its mineral resources, regardless of the fact that the composition of MSRs from different sources differs slightly [7]. Researchers have investigated a number of approaches for recovering copper from copper-containing waste in recent years. On the basis of their principles, these methods can be classified into three categories, namely, pyrometallurgy, hydrometallurgy, and flotation. Unlike hydrometallurgy, however, pyrometallurgy [8–10] does not make sense for the treatment of MSR, because organic components in MSR can be volatilized or cleaved at high temperatures. Additionally, flotation cannot recover all the copper from MSR due to its complex composition [11–14]. Hydrometallurgy is therefore used in this study as an effective and low-cost method. The hydrogen peroxide as a safe, effective, powerful and versatile oxidant is widely used in hydrometallurgical processes. In Table 1, reported studies related to the hydrometallurgical leaching of copper with H_2O_2 are listed. In acidic solution, H_2O_2 is one of the most powerful oxidants known stronger than chlorine, chlorine dioxide and potassium permanganate. The oxidizing capacity of hydrogen peroxide is so

* Corresponding author.
E-mail address: xingpf@smm.neu.edu.cn (P. Xing).

https://doi.org/10.1016/j.cjche.2023.02.007
1004-9541/

Table 1
Leaching of Cu from different wastes

Material	Leaching agent	Leaching field of Cu	Ref.
Waste Pb-free solder	$HCl–H_2O_2$		[15]
Magnet scrap	$HCl–H_2O_2$–LIX 84I	97	[16]
Printed circuit boards	$HCl–H_2O_2$	98	[17]
Printed circuit boards	$H_2SO_4–H_2O_2$	100	[18]
Automobile shredder residue	$H_2SO_4–H_2O_2–Fe^{3+}$	78	[19]
Waste printed circuit boards	$H_2SO_4–H_2O_2$	90	[20]
Waste printed circuit boards	Glycine–H_2O_2	94	[21]
Waste printed circuit boards	Glycine–H_2O_2	96.5	[22]
Pure copper discs	Glycine–H_2O_2		[23]

strong that it is considered a highly reactive oxygen species. Since the dissolution of copper requires an acidic environment, HCl [15–17] and H_2SO_4 [18–20] are widely used in leaching copper from different waste materials. The oxidation and dissolution of copper was investigated using hydrogen peroxide as oxidizer and glycine as a complexing agent [21–23]. As for Cu leaching from MSR, Ren *et al.* [24] compared the effects of particle size and hydrogen peroxide on the leaching effect of copper and found that a decrease in particle size was more favorable to the leaching of copper, but the reaction mechanism was not investigated in detail.

By learning from other methods of leaching copper from copper-containing wastes and as a supplement to the study of copper extraction from MSR, hydrogen peroxide was used as the leaching reagent in this paper. This study's experiments were divided into two parts. To begin, the optimized conditions for the extraction of copper from MSR by hydrogen peroxide were explored. Then the corresponding leaching kinetics were thoroughly investigated, which will provide direction for industrial copper regeneration and recovery.

2. Material and Methods

2.1. Material and analysis

MSR that has been hydrolyzed and plate pressed was provided by Hoshine Silicon Co., Ltd. in China. Before treatment, the characterization was conducted as shown in Fig. 1. The particle size distribution of MSR reveals the fine characteristics of the particles with an average size of 28.15 μm (Fig. 1(a)). To investigate the group structure of MSR, the FTIR of MSR was conducted (Fig. 1(b)). Absorption bands at 772.11 cm^{-1} and 1037.84 cm^{-1} in MSR before leaching were Si—O—Si bond [25,26]. The H—O—H bond was identified at 1740.34 cm^{-1}, while the C—H peak was identified at 2977.07 cm^{-1} [27,28]. The presence of copper chloride can be clearly seen in Fig. 1(c). Based on chemical analysis, the bulk density is 0.5283 $g·cm^{-3}$, with mass contents of 28% silicon, 5.6% copper, 2.3% iron, and 64.1% organics (obtained by differential weight method). All experiments reagents of analytical grade, including H_2O_2, HCl, HNO_3, $HClO_4$, and HF, were purchased from Sinopharm Chemical Reagent Co., Ltd. in Shenyang of China.

2.2. Experimental procedure

Before the analyses and experiments, MSR were ground to powder in an agate mortar and passed through a mesh 50 μm sieve. Following that, leaching experiments were carried out using a magnetic stirrer apparatus, which consisted primarily of a glass beaker placed on a thermostatic hot water bath and equipped with a magnetic stirrer. Approximately 2 g of the sample was immersed in solution for varying lengths of time at the desired concentration, temperature, liquid–solid ratio and stirring speed. A certain amount of HCl was added to keep the pH < 3 during the experiment. After leaching, filtering was conducted. The solution was preserved for analysis and the leaching residue was dried in a vacuum oven at 343 K for 12 h.

2.3. Analysis and characterization

The morphologies and microstructures of the samples were observed using a field emission scanning electron microscope (SEM, QUANTA 200, FEI, USA). To characterize metal impurities, an energy-dispersive X-ray spectrometer (EDS) installed in the SEM was used. The samples were coated with Au prior to SEM. The voltage for EDS was 15.00 kV. The structure of the samples was detected by Fourier transform infrared spectrometer (FTIR, Nicolet iS20, Thermo Scientific, Germany) and the X-ray diffraction pattern (XRD, SmartLab-SE, Rigaku, Japan). The concentration of Cu was analyzed by using inductively coupled plasma mass spectrometry (ICP-MS, 7700e, Agilent, USA).

3. Results and Discussion

3.1. Extraction of Cu from MSR

MSR contains copper primarily in the form of $CuCl_2$, CuCl and Cu. The copper mass content in $CuCl_2$ is 3.25%. The copper mass content of CuCl and Cu is 2.38%. Cu and CuCl are generally incapable of dissolving in acids due to the low reducibility [29], whereas they are more likely to dissolve in the presence of H_2O_2 as an oxidizing reaction. The chemical reaction of Cu extraction in H_2O_2 solution are Eqs. (1) and (2):

$$H_2O_{2(l)} + Cu_{(s)} + 2H^+_{(l)} = Cu^{2+}_{(l)} + 2H_2O_{(l)} \quad (1)$$

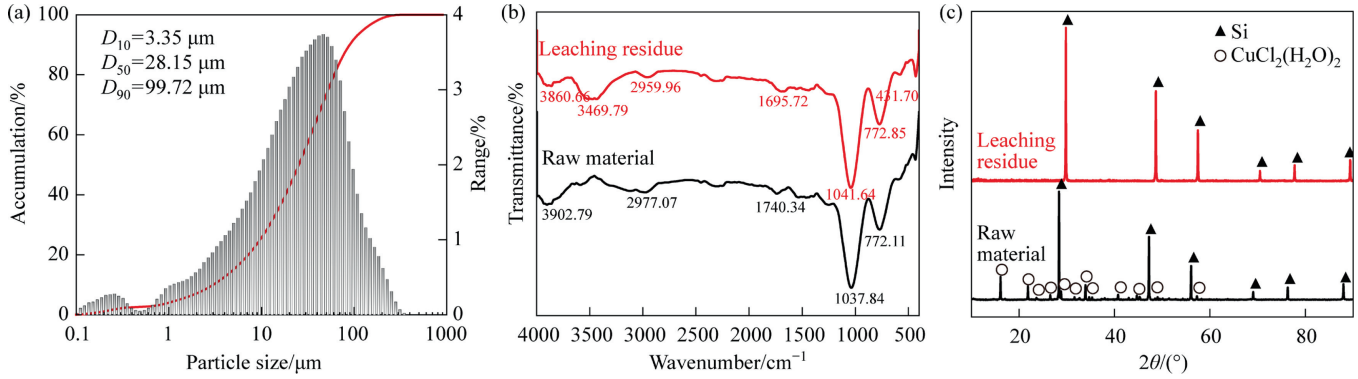

Fig. 1. Characterization of MSR: (a) the particle size distribution, (b) the Fourier transform infrared spectroscopy, (c) the X-ray diffraction pattern.

$$2CuCl_{(s)} + 2H^{+}_{(l)} + H_2O_{2(l)} = 2Cu^{2+}_{(l)} + 2H_2O_{(l)} + 2Cl^{-}_{(l)} \quad (2)$$

The extraction efficiency of Cu could be defined as follows:

$$X = \frac{C_1 \times V}{C_2 \times M} \times 100\% \quad (3)$$

where X is the extraction efficiency of Cu (%); V is the volume of the leaching solution (ml); M is the mass of MSR (g); C_1 refers to the concentration of copper in leaching solution (g·ml^{-1}), and C_2 refer to the percentages of copper in MSR (%).

MSR leaching experiments with H_2O_2 addition were conducted using a variety of experimental parameters, including H_2O_2 concentration, leaching temperature, liquid–solid ratio, and stirring speed with the same holding time of 90 min. The effects of these leaching parameters on the Cu extraction efficiency were studied, as shown in Fig. 2(a)–(d). The effect of H_2O_2 concentration on Cu extraction is shown in Fig. 2(a). The extraction efficiency of Cu was found to be highly dependent on the concentration of H_2O_2. When the H_2O_2 concentration was low, the extraction efficiency increased sharply as the H_2O_2 concentration increased. However, when the H_2O_2 solution concentration is above 1.875 mol·L^{-1}, further increase had little effect on the Cu extraction efficiency. The effect of leaching temperature on Cu recovery was investigated in Fig. 2(b). The extraction efficiency of Cu was found to be 92.5% at a leaching temperature of 313 K. As the temperature increased, the Cu extraction efficiency improved slightly. The H_2O_2 was temperature sensitive during the leaching process. At high temperatures, the decomposition reaction of H_2O_2 will take place. Therefore, the choice of temperature is particularly important. As a result, 323 K was chosen as the leaching temperature for the following experiments. The effect of liquid–solid ratio on Cu recovery was investigated in Fig. 2(c). At low liquid–solid ratios, the extraction efficiency of Cu increased with liquid–solid ratio increased, but there was a slight decrease in Cu extraction efficiency after 20 ml·g^{-1}. These findings demonstrated that the liquid–solid ratio significantly improved Cu extraction in these experiments. The low liquid–solid ratio prevents contact between MSR powders and H_2O_2 solution. Additionally, the high viscosity complicates ion diffusion, resulting in a low Cu extraction efficiency. When the liquid–solid ratio is too high, the composition in the liquid is not uniformly distributed, and a series of hydrolytic condensation reactions occur in MSR to limit the contact interface between Cu and H_2O_2. At the same time, the high liquid–solid ratio has a negative impact on subsequent copper enrichment. As a result, when considering both chemical consumption and extraction efficiency of Cu for industrial applications, the liquid–solid ratio was suggested to be 20 ml·g^{-1}. The effect of stirring speed on Cu extraction was investigated in Fig. 2(d). As can be seen, the extraction efficiency of Cu only increased slightly as the stirring speed increased. This suggests that diffusion may not be the reaction's limiting step.

In conclusion, the optimal experimental conditions (1.875 mol·L^{-1} of H_2O_2 concentration, 323 K of temperature, 20 ml·g^{-1} of liquid–solid ratio, and 300 r·min^{-1} of stirring speed) were obtained with the Cu extraction efficiency of approximately 98.5%.

3.2. Kinetics analysis for Cu extraction

The H_2O_2 concentration and leaching temperature were discovered to be the most effective parameters on the extraction efficiency of Cu. The results are presented in Fig. 3. The Cu responds rapidly with H_2O_2 and achieves a constant efficiency after a period

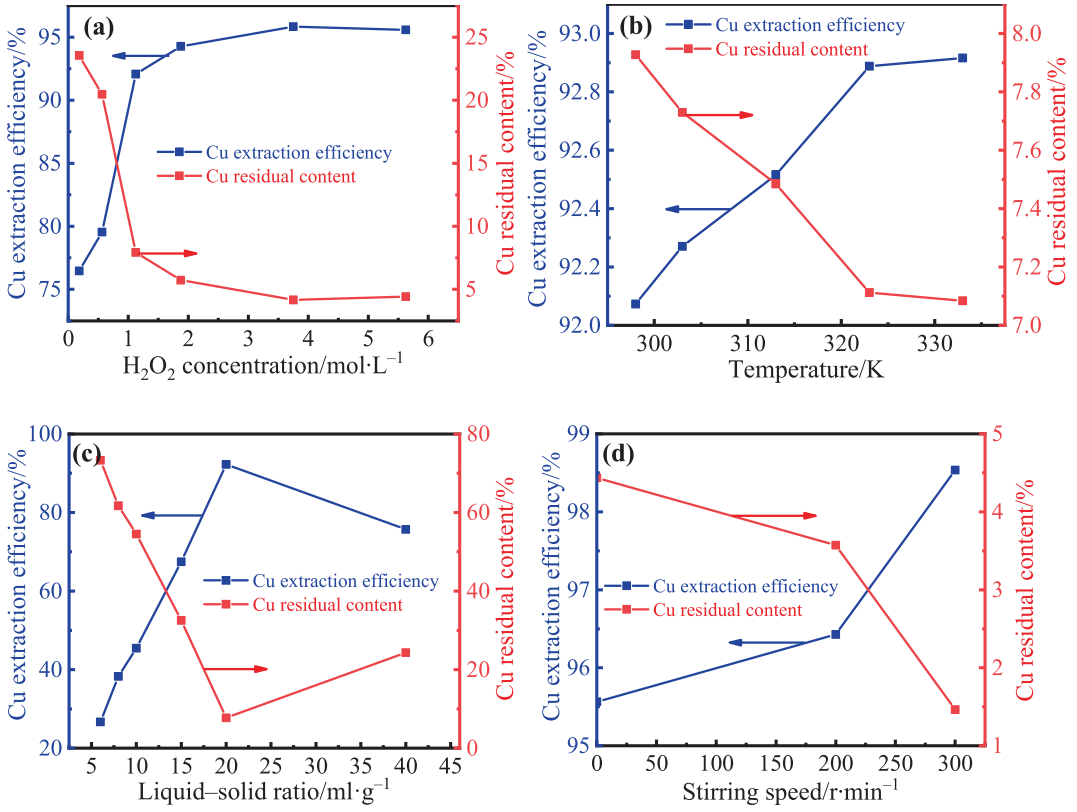

Fig. 2. The relations between Cu extraction efficiency and leaching parameters: (a) H_2O_2 concentration (298 K of temperature, 20 ml·g^{-1} of liquid–solid ratio and 0 r·min^{-1} of stirring speed), (b) leaching temperature (1.125 mol·L^{-1} of H_2O_2 concentration, 20 ml·g^{-1} of liquid–solid ratio and 0 r·min^{-1} of stirring speed), (c) liquid–solid ratio (1.125 mol·L^{-1} of H_2O_2 concentration, 298 K of temperature and 0 r·min^{-1} of stirring speed), (d) stirring speed (1.875 mol·L^{-1} of H_2O_2 concentration, 323 K of temperature, and 20 ml·g^{-1} of liquid–solid ratio).

of time. Furthermore, at higher temperatures and concentrations, the reaction time to reach steady is shorter. It should also be noted that the low extraction efficiency of Cu at low concentrations is due to a lack of hydrogen peroxide. During the reaction, Cu^{2+} can catalyze the decomposition of hydrogen peroxide [30]. The shrinking core model was used to analyze the kinetics of Cu extraction with different times for temperature and H_2O_2 concentration in order to better understand the leaching mechanism.

The reaction in MSR is solid–liquid reaction. No solid phase product or solid inert residues are generated. The process includes simple copper chloride dissolution, which is primarily controlled by diffusion, and electrochemical dissolution of copper and cuprous chloride, which is primarily controlled by chemical reaction and diffusion. In this study, the shrinking core model with surface chemical reaction and diffusion through product layer, as well as a new variant shrinking core model [31], were evaluated for kinetic data analysis.

Chemical reaction control:

$$1-(1-X)^{1/3}=k_1t \tag{4}$$

Product layer diffusion control:

$$1-\frac{2}{3}X-(1-X)^{2/3}=k_2t \tag{5}$$

Interfacial transfer and product layer diffusion both control:

$$\frac{1}{3}\ln(1-X)-1+(1-X)^{-1/3}=k_3t \tag{6}$$

where X is the extraction efficiency of Cu (%), t is the leaching time (min), and k_n is the apparent constant of each reaction control (dimensionless).

The reaction rate is usually determined by three variables: temperature (T, K), H_2O_2 concentration ($C_{H_2O_2}$, mol·L^{-1}) and extraction efficiency of Cu (X, %). k is frequently determined using the n order Arrhenius equation, expressed as Eq. (7), based on the reaction temperature and H_2O_2 concentration for the shrinking core model.

$$k=AC_{H_2O_2}^{n}\exp(-E_a/RT) \tag{7}$$

where A is the pre-exponential factor (min^{-1}); n is the experimental reaction order to the H_2O_2 concentration; E_a is activation energy (J·mol^{-1}); R is the universal gas constant, which is 8.314 (J·(mol·K)$^{-1}$); and the pre-exponential factor A corresponds to the frequency and orientation of molecule collisions.

The reaction process of Cu and H_2O_2 in MSR can be divided into two stages, as shown in Fig. 3. And because the reaction rates of the two stages differ, the control steps may also differ. As a result, in this study, the kinetic models of the two stages are discussed separately.

Fitting Eqs. (4)–(6) as a function of time determined the controlling steps of the leaching reaction for the shrinking core model. The experimental data from 298, 303, 313, 323, and 333 K were entered into Eqs. (4)–(6). These expressions were then plotted and fitted to the leaching time. The best match between the experimental data and the chemical reaction control can be seen by comparing Fig. 4(a)–(c), as evidenced by the highest R^2 value. The results show that the copper leaching process with H_2O_2 addition at first stage fits the chemical reaction controlled model. Fig. 4 (d)–(f) show the results of fitting the experimental data of second stage of the copper extraction process to Eqs. (4)–(6). The new variant shrinking core model show the best correlation between the experimental data with Eq. (6), meaning that the leaching process of copper in second stage is controlled by both interfacial transfer and product layer diffusion.

Eq. (8) was produced from the natural logarithm of Eq. (7):

$$\ln k=\ln A+n\ln C_{H_2O_2}-E_a/RT \tag{8}$$

The plot of ln$k$ *versus* 1000/T as a straight line with a slope of $-E_a/R$ if the H_2O_2 concentration remained constant is shown in A1 of Supplemental Material. The lines' slopes were calculated to be –2.4789 and –2.2092. The apparent activation energy was calculated to be 20.609 kJ·mol^{-1} at first stage and 18.367 kJ·mol^{-1} at second stage. In this way, the values less than 20 kJ·mol^{-1} indicate diffusion-controlled processes [32,33], which coincides with our data at second stage. If the temperature remained constant, the plot of ln$k$ *versus* ln$C_{H_2O_2}$ was a straight line with a slope n, as shown in Eq. (8). The H_2O_2 reaction order at first stage was 0.4747 (shown in A2 of Supplemental Material) and the H_2O_2 reaction order of 1.4515 at second stage was also obtained (shown in A3 of Supplemental Material).

When both E_a and n were known, the pre-exponential factor A of 55.1061 at first stage and 2.8649 × 10^6 at second stage could be easily determined according to Eq. (8). With the values of E_a and n at two stages already determined, these parameters were entered into Eq. (7). Following that, in conjunction with Eqs. (4) and (6), the kinetics equation was produced as Eq. (9):

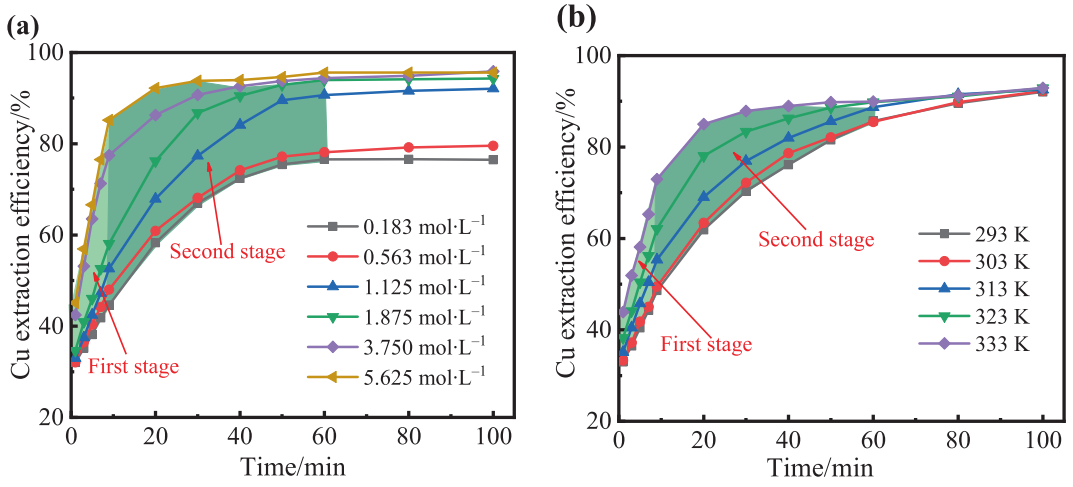

Fig. 3. Cu extraction efficiency in H_2O_2 at (a) different concentration (temperature of 298 K, 20 ml·g^{-1} of liquid–solid ratio and 0 r·min^{-1} of stirring speed), (b) different temperature (1.125 mol·L^{-1} of H_2O_2 concentration, 20 ml·g^{-1} of liquid–solid ratio and 0 r·min^{-1} of stirring speed).

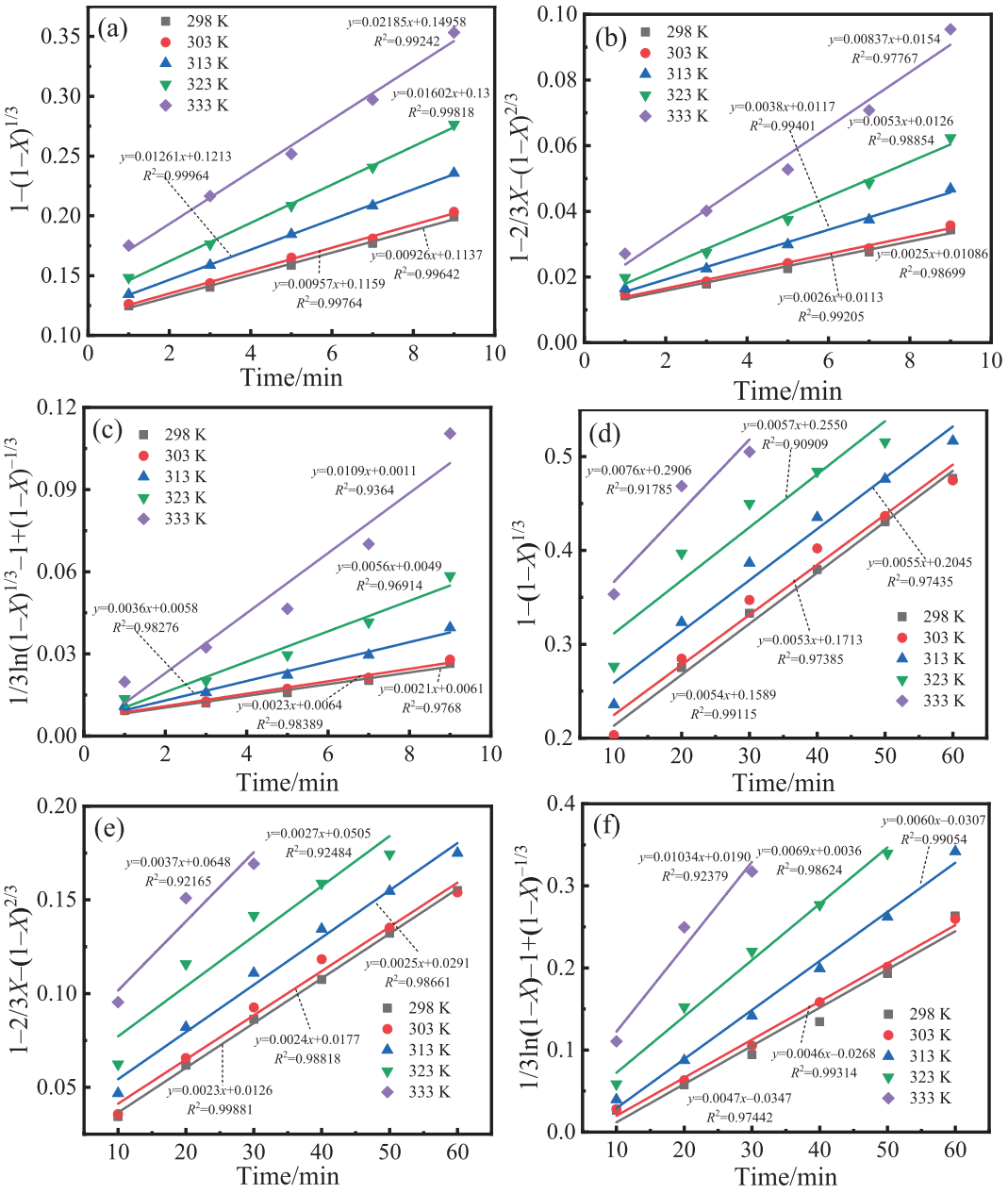

Fig. 4. Fitting of experimental data for different temperatures in the first stage: (a) plot of $1-(1-X)^{1/3}$ *vs* time, (b) plot of $1-2/3X-(1-X)^{2/3}$ *vs* time, (c) plot of $1/3\ln(1-X)-1+(1-X)^{-1/3}$ *vs* time, and the second stage: (d) plot of $1-(1-X)^{1/3}$ *vs* time, (e) plot of $1-2/3X-(1-X)^{2/3}$ *vs* time, (f) plot of $1/3\ln(1-X)-1+(1-X)^{-1/3}$ *vs* time.

$$\begin{cases} 1-(1-X)^{\frac{1}{3}} = \left(33.39C_{H_2O_2}^{0.47}\exp\left(-\dfrac{20610}{RT}\right)\right)t & \text{(first stage)} \\ \dfrac{1}{3}\ln(1-X)-1+(1-X)^{-\frac{1}{3}} = \left(2.86\times10^{6}C_{H_2O_2}^{1.45}\exp\left(-\dfrac{18267}{RT}\right)\right)t & \text{(second stage)} \end{cases} \quad (9)$$

Eq. (9) can be used to predict the relationship between Cu extraction efficiency X and reaction time t at the two stages of Cu extraction from MSR in H_2O_2 solution within an acceptable error under certain experimental conditions. In this regard, the developed Eq. (9) proved semi-empirical mathematical model implying that any further increase in concentration or temperature does not improve Cu extraction efficiency solely through H_2O_2 leaching.

3.3. Analysis of leaching residue

FTIR was conducted after leaching, as shown in Fig. 1(b). In the FTIR of leaching residue, Si—O—Si peak could still be observed with only a slight shift. The Si—O—Si bending vibration peak of 431.70 cm^{-1} and the isolated silanols or terminal silanols of 3469.79 cm^{-1} have been added. This indicates that the residue was clearly oxidized and hydrolyzed. The XRD patterns of the solids after leaching are shown in Fig. 1(c). It is clear that the copper in MSR is largely extracted.

SEM of the MSR before and after leaching are presented in Fig. 5. The particle size of MSR is not uniform. The MSR exhibits the aggregation structure. Copper is discrete on the surface and within the particles, as evidenced by the EDS results in Fig. 5(a). The aggregation structure would effectively result in a passive effect for the extraction of copper located on the blind spots. In other words, the copper contained in the inner of large particles or at particle interfaces is hard to react with hydrogen peroxide. As shown in Fig. 5(b), the number and size of aggregation structures are both reduced. This is due to the use of magnetic stirring in the reaction process. On the other hand, the continuous escape of

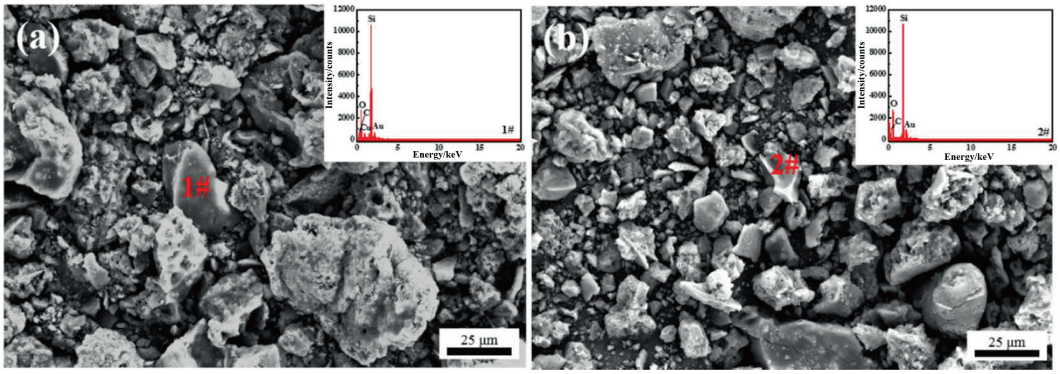

Fig. 5. SEM images of the MSR: (a) before leaching, (b) after leached for 100 min with H_2O_2 under optimal conditions.

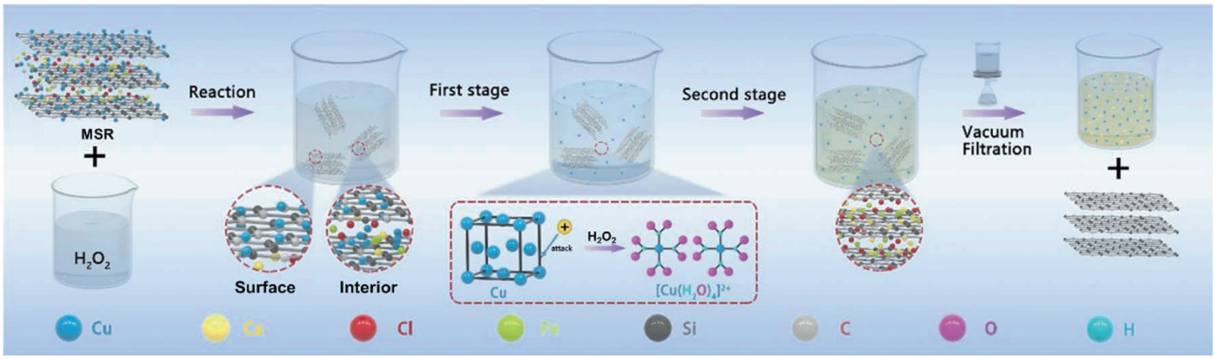

Fig. 6. Schematic illustration of copper extraction from MSR.

oxygen produced by the decomposition of hydrogen peroxide leads to the breaking of large particles in MSR into small particles. This procedure makes it easier to recover the copper within the particles. Meanwhile, EDS results also show that copper has been largely leached.

3.4. Mechanism of Cu recovery from organosilicon sludge

The extraction of Cu under the above optimized conditions reached over 98%, proving that Cu was leached from both the surface and the interior of MSR. According to the kinetics discussed in Section 3.2, the mechanism of copper extraction is graphically and vividly illustrated in Fig. 6. MSR particles are continuously dissolved in the solution. In the first stage, the leaching mainly removes the copper particles adhering on the surface of MSR particles, of which the copper particles become shrinking until disappear. This process is mainly controlled by an electrochemical reaction in which large amounts of copper ions are produced. Electron transfer is necessary for dissolution of copper. The second stage occurs mainly inside the MSR particles and is controlled by both interfacial transfer and product layer diffusion. The Cu^{2+} produced in the first step catalyzes the decomposition of hydrogen peroxide to produce oxygen. The continuous overflow of oxygen causes the MSR particles to "bounce" up and down, thus facilitating the entrance of the solution into the MSR particles and enhancing diffusion and material transfer. Although the Cu in this study reacted rapidly with H_2O_2 and the presence of H_2O_2 facilitated diffusion, Cu was not fully extracted from interior particles due to the interference effect caused by particle aggregation.

4. Conclusions

It has been demonstrated in this study that a Cu extraction process with H_2O_2 would achieve complete recovery of copper from MSR. The process has a high separation and recovery efficiency to extract Cu from MSR and does not cause any adverse impacts on the environment. The optimum parameters were obtained as hydrogen peroxide concentration of 1.875 $mol \cdot L^{-1}$, leaching temperature of 323 K, liquid–solid ratio 20 $ml \cdot g^{-1}$ and stirring speed of 300 $r \cdot min^{-1}$, with the copper extraction efficiency of 98.5%. The copper extraction process was found to be divided into two stages. The first stage was controlled by a chemical reaction. The second stage was controlled by both interfacial transfer and product layer diffusion, mainly for the dissolution of copper chloride. The particle size decreased after the reaction and hollows appeared on the surface of the particles, caused by the combined effect of hydrogen peroxide decomposition and agitation. The reaction mechanism showed that copper particles mainly existed on the surface and at the interior of MSR particles. The copper particles on the surface of the MSR were removed in the first stage of the reaction as electrochemical dissolution, and in the second stage a simple dissolution reaction of copper chloride primarily occurred. The conclusions from this study will provide practical guidance for recycling MSR. And the leaching residue can be used for the subsequent synthesis of silicon carbide nanowires. This study realizes MSR's harmless treatment.

Data Availability

Data will be made available on request.

Declaration of Competing Interest

The authors declare that they have no known competing financial interests or personal relationships that could have appeared to influence the work reported in this paper.

Acknowledgements

This work was supported by the National Key Research and Development Program of China (2018YFC1901804 and 2018YFC1901805) and the National Natural Science Foundation of China (21978045 and U1902219).

Supplementary Material

Supplementary material to this article can be found online at https://doi.org/10.1016/j.cjche.2023.02.007.

References

[1] F. Zhu, X.Y. Hu, L.H. Kong, X.J. Peng, Calcium sulfide-organosilicon complex for sustained release of H_2S in strongly acidic wastewater: Synthesis, mechanism and efficiency, *J. Hazard. Mater.* 421 (2022) 126745.
[2] H. Osip, C. Czosnek, J.F. Janik, J. Marchewka, M. Sitarz, Amorphous silicon oxynitride-based powders produced by spray pyrolysis from liquid organosilicon compounds, *Materials* 14 (2) (2021) 386.
[3] J.J. Zuckerman, The direct synthesis of organosilicon compounds, *Adv. Inorg. Chem. Radiochem.* 6 (1964) 383–432.
[4] J.H. Downing, J.W. Iii, T.K. Ioannou, Preparation of reaction mass for the production of methylchlorosilane, China Pat., CA1158629A (1982).
[5] L. Hong, Study on the application of organosilicon high-boiling by-products to ready-mixed waterproof mortar, *J. Fujian Univ. Technol.* 12 (2014) 42–46. (in Chinese)
[6] M.S. McLachlan, A. Kierkegaard, M. Radke, A. Sobek, A. Malmvärn, T. Alsberg, J. A. Arnot, T.N. Brown, F. Wania, K. Breivik, S.H. Xu, Using model-based screening to help discover unknown environmental contaminants, *Environ. Sci. Technol.* 48 (13) (2014) 7264–7271.
[7] G. Singh, P. Satija, A. Singh, P. Diksha, S. Suman, S.S. Mohit, Azo dye featuring triazole appended organosilicon multifunctionalized sensor: Paradigm for detection of Cu^{2+} and Fe^{2+} ions, *Mater. Chem. Phys.* 249 (2020) 123005.
[8] V. Sivakumar, F. Chandrasekarana, G. Swaminathana, P.G. Rao, Towards cleaner degreasing method in industries: Ultrasound-assisted aqueous degreasing process in leather making, *J. Clean. Prod.* 17 (1) (2009) 101–104.
[9] V. Sivakumar, R.P. Poorna, P.G. Rao, B.V. Ramabrahmam, G. Swaminathana, Power ultrasound in fatliquor preparation based on vegetable oil for leather application, *J. Clean. Prod.* 16 (4) (2008) 549–553.
[10] V. Sivakumar, V.V. Ravi, P.G. Rao, G. Swaminathana, Studies on the use of power ultrasound in solid–liquid myrobalan extraction process, *J. Clean. Prod.* 15 (18) (2007) 1813–1818.
[11] K. Haga, W. Tongamp, A. Shibayama, Investigation of flotation parameters for copper recovery from enargite and chalcopyrite mixed ore, *Mater. Trans.* 53 (4) (2012) 707–715.
[12] Q. Dehaine, L.O. Filippov, I.V. Filippova, I.V. Filippovac, L.T. Tijsselingd, H.J. Glassa, Novel approach for processing complex carbonate-rich copper-cobalt mixed ores *via* reverse flotation, *Miner. Eng.* 161 (2021) 106710.
[13] Y.F. Mu, Y.J. Peng, Selectively depress copper-activated pyrite in copper flotation at slightly alkaline pH, *Min. Metall. Explor.* 38 (2) (2021) 751–762.
[14] H.P. Dong, D.K. He, F.L. Wang, SMOTE-XGBoost using tree Parzen estimator optimization for copper flotation method classification, *Powder Technol.* 375 (2020) 174–181.
[15] S. Kim, J.C. Lee, K.S. Lee, K. Yoo, R.D. Alorro, Separation of tin, silver and copper from waste Pb-free solder using hydrochloric acid leaching with hydrogen peroxide, *Mater. Trans.* 55 (12) (2014) 1885–1889.
[16] A.K. Nayak, B. Behera, K. Sarangi, M.K. Ghosh, S. Basu, Process flowsheet development for separation of Sm, Co, Cu, and Fe from magnet scrap, *ACS Omega* 6 (1) (2021) 188–196.
[17] Z.K. Wang, S. Guo, C. Ye, Leaching of copper from metal powders mechanically separated from waste printed circuit boards in chloride media using hydrogen peroxide as oxidant, *Procedia Environ. Sci.* 31 (2016) 917–924.
[18] C.J. Oh, S.O. Lee, H.S. Yang, T.J. Ha, M.J. Kim, Selective leaching of valuable metals from waste printed circuit boards, *J. Air Waste Manag. Assoc.* 53 (7) (2003) 897–902.
[19] F. Ferella, I.D. Michelis, A. Scocchera, M. Pelino, F. Vegliò, Extraction of metals from automotive shredder residue: Preliminary results of different leaching systems, *Chin. J. Chem. Eng.* 23 (2) (2015) 417–424.
[20] I. Birloaga, I.D. Michelis, F. Ferella, M. Buzatu, F. Veglio, Study on the influence of various factors in the hydrometallurgical processing of waste printed circuit boards for copper and gold recovery, *Waste Manag.* 33 (4) (2013) 935–941.
[21] Y.H. Han, X. Yi, R. Wang, J. Huang, J. Shu, Copper extraction from waste printed circuit boards by glycine, *Sep. Purif. Technol.* 253 (2020) 117463.
[22] H. Li, E.A. Oraby, J.J. Eksteen, Extraction of copper and the co-leaching behavior of other metals from waste printed circuit boards using alkaline glycine solutions, *Resour. Conserv. Recycl.* 154 (2020) 104624.
[23] S. Seal, S.C. Kuiry, B. Heinmen, Effect of glycine and hydrogen peroxide on chemical-mechanical planarization of copper, *Thin Solid Films* 423 (2) (2003) 243–251.
[24] H.T. Ren, Q.U. Hu, H. Cao, J. Zhao, B. Liu, Q.Y. Liu, Small pilot study on optimization of copper extraction process from organosilicon slurry, *China Chem. Trade* 10 (2018) 96. (in Chinese)
[25] Y.B. Xiao, Y. Wang, G. Luo, S. Bai, Using hydrolysis of silicon tetrachloride to prepare highly dispersed precipitated nanosilica, *Chem. Eng. J.* 283 (2016) 1–8.
[26] P.R. Pinto, L.C. Mendes, M.L. Dias, C. Azuma, Synthesis of acrylic-modified sol–gel silica, *Colloid Polym. Sci.* 284 (5) (2006) 529–535.
[27] F. Yan, J.G. Jiang, S.C. Tian, Z.W. Liu, J. Shi, K.M. Li, X.J. Chen, Y.W. X u,, A green and facile synthesis of ordered mesoporous nanosilica using coal fly ash, *ACS Sustain. Chem. Eng.* 4 (9) (2016) 4654–4661.
[28] S. Cerveny, G.A. Schwartz, J. Otegui, J. Colmenero, J. Loichen, S. Westermann, Dielectric study of hydration water in silica nanoparticles, *J. Phys. Chem. C* 116 (45) (2012) 24340–24349.
[29] A. Janin, L. Coudert, G. Mercier, J.F. Blais, Copper extraction and recovery from alkaline copper quaternary and copper azole treated wood using sulfuric acid leaching and ion exchange or electrodeposition, *J. Clean. Prod.* 279 (2021) 123687.
[30] S.C. Yang, K.X. Wei, W.H. Ma, K. Xie, J. Wu, L. Yun, Kinetic mechanism of aluminum removal from diamond wire saw powder in HCl solution, *J. Hazard. Mater.* 368 (2019) 1–9.
[31] T.M. Florence, The production of hydroxyl radical from hydrogen peroxide, *J. Inorg. Biochem.* 22 (4) (1984) 221–230.
[32] R.L. Zhang, X.F. Zhang, S.Z. Tang, A.D. Huang, Ultrasound-assisted HCl–NaCl leaching of lead-rich and antimony-rich oxidizing slag, *Ultrason. Sonochem.* 27 (2015) 187–191.
[33] H. Chen, K. Morita, X.D. Ma, Z.Y. Chen, Y. Wang, Boron removal for solar-grade silicon production by metallurgical route: A review, *Sol. Energy Mater. Sol. Cells* 203 (2019) 110169.